

## NOTE AND CORRESPONDENCE

---

TAO, Vol.5, No.4, 611-623, December 1994

### Initial Investigation of the May 24, 1994 Hualien and June 5, 1994 Nanao Earthquakes

KUO-FONG MA<sup>1</sup> and MASAYUKI KIKUCHI<sup>2</sup>

(Manuscript received 24 June 1994, in final form 3 November 1994)

#### ABSTRACT

We investigate the characteristics of the May 24, 1994 Hualien and June 5, 1994 Nanao earthquakes using the long period P-wave data recorded by the IRIS (Incorporated Research Institution for Seismology). The solution based on long period P waves gives a mechanism with dip=23.6°, rake=-31.4° and strike=135.3°, and a seismic moment of  $9.0 \times 10^{25} \sim 1.3 \times 10^{26}$  dyne-cm ( $M_w=6.6 \sim 6.7$ ) for the Hualien earthquake; and with dip=62.6°, rake=25.0° and strike=293.2°, and a seismic moment of  $3.73 \times 10^{25}$  dyne-cm ( $M_w=6.4$ ) for the Nanao earthquake. The source time-function of the May 24, 1994 Hualien earthquake consisted of a main event with a time duration of 8 sec followed by two small subevents extending the total duration of the source time-function to 35 sec. This long duration of source time function and the difference between  $M_s$  and  $m_b$  suggest the Hualien earthquake was a slow earthquake. The source time function of the June 5, 1994 Nanao earthquake had a time duration of 6 sec and was rather simple compared with Hualien earthquake. The average slips on the fault for the Hualien and Nanao earthquakes were 40~92.3 cm and 51.8 cm, respectively. The stress drops of the two intra-plate events were comparable to those of most large earthquake.

(Key words: IRIS, Slow earthquake, Stress drops)

#### 1. INTRODUCTION

The Hualien earthquake occurred on May 24, 1994, 04h00m44.85s GMT (CWB Earthquake Report Center). The epicenter determined from the local seismic network, the Central Weather Bureau Seismographic Network (CWBSN), was at the longitude of 122.61°E, latitude of 23.83°N and the depth of 2.9 km. The location of the earthquake determined by the United

---

<sup>1</sup> Institute of Geophysics, National Central University, Chung-Li, Taiwan, R.O.C.

<sup>2</sup> Department of Physics, Yokohama City University, Yokohama 236, Japan

States Geological Survey, the National Earthquake Information Center using the broadband IRIS (Incorporated Research Institution for Seismology) data was  $122.3^{\circ}\text{E}$  in longitude and  $24.0^{\circ}\text{N}$  in latitude. About two weeks after the Hualien earthquake, a Nanao earthquake with a very similar magnitude occurred on June 5, 1994, 01h09m34.4s GMT (CWB Earthquake Report Center). The epicenter determined from the CWBSN was at the longitude of  $121.84^{\circ}\text{E}$ , latitude of  $24.46^{\circ}\text{N}$  and the depth of 5.3 km while the IRIS reported a longitude of  $121.9^{\circ}\text{E}$ , latitude of  $24.5^{\circ}\text{N}$  and a depth of 15.9 km. This earthquake was about 150 km to the northwest of the Hualien earthquake.

The Hualien and Nanao earthquakes were unique since they both occurred near the boundary where the Phillipine Sea Plate subducts into the Eurasia Plate (Figure 1). The tectonic structure in this region had long been a subject of debate. Wu (1970) suggested that a transform fault was involved in the subduction feature of the Ryukyu Trench. However, Bowin and others (1978) suggested the existence of a continuous Ryukyu Trench structure to northern Taiwan. These two earthquakes provide a good opportunity to understand the complex tectonic features in this region. However, for the complete understanding of the tectonic implications of the two earthquakes, it is necessary to consider all of the available seismic data. In the present study, we did not attempt to understand the tectonic implications of the two earthquakes. However, in view of the uniqueness of the two earthquakes, in addition to the tectonic studies, it became worthwhile to understand the characteristics of the earthquakes as they would then provide important seismic information of the earthquakes for further studies.

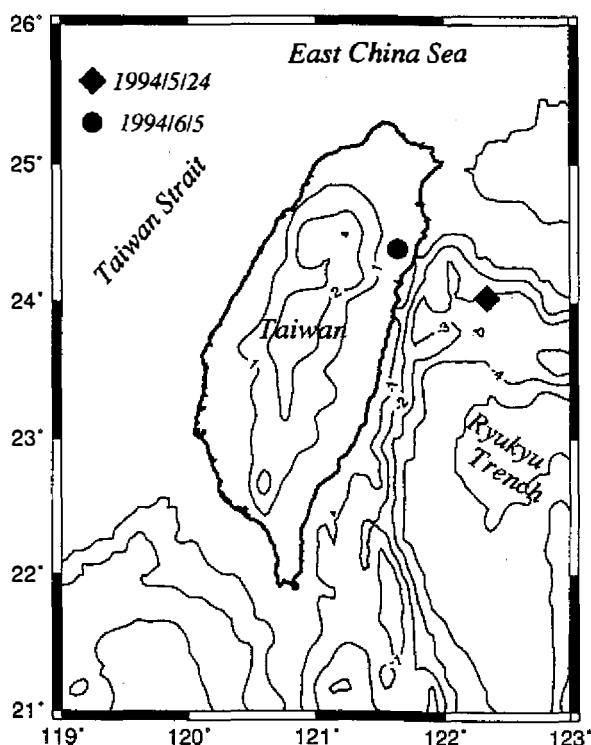


Fig. 1. Locations of the May 24, 1994 Hualien and June 5, 1994 Nanao earthquakes. The contour lines indicate the bathymetry in km.

The focal mechanism of an earthquake is an important parameter from which to understand the characteristics of the earthquake. However, the first-motion mechanisms of an earthquake are difficult to determine due to the sparse distribution of the first motions of offshore events. The open access of regional distance waveforms of the IRIS Data Management Center in USA offers an opportunity to utilize regional waveform data to determine focal mechanisms, especially if the local waveform data are not yet available or if the first-motion data are not good enough for mechanism determination. Since the S-wave for most regional stations are clipped or are too complex to distinguish the source or structure effect, the long-period S-wave is not considered in the present study. In this paper, the method developed by Kikuchi and Kanamori (1989) to invert the regional P-wave waveform is applied to obtain the mechanisms and seismic moments of these two earthquakes. The quick mechanism and seismic moment determination of the earthquakes can help us to have a quick understanding of the characteristics of the earthquakes and provide other information such as fault area, stress drop and average slip on the fault for further study on the earthquake.

## 2. FOCAL MECHANISM AND SOURCE TIME FUNCTION

In this study, the focal mechanisms and seismic moments were determined using the data collected by the IRIS Data Management Center soon after the earthquakes. All the seismograms are deconvolved to ground motion displacements. The long period body wave inversion method developed by Kikuchi and Kanamori (1989) was used to invert these records and determine the mechanisms. This method is an extension of the multiple deconvolution method of Kikuchi and Kanamori (1982, 1986). The observed seismograms are matched by synthetics computed for a sequence of subevents distributed on a fault plane. Green's functions for five independent moment tensor elements are computed, and the subevents are represented by a linear combination of them. By minimizing the difference between the observed and synthetic seismograms, we determine the moment tensor or mechanism of the event.

### 2.1 The 1994 May 24, Hualien Earthquake

15 of the IRIS stations were used in this study. As the P-wave waveforms of these stations were generally rather complex as shown in Figure 2, it was difficult to distinguish source effect from structure effect. The parameters of these 15 stations respect to the epicenter is listed in Table 1. To model the source time function of the earthquake, therefore, a single source with a trapezoidal time function ( $t_1$ ,  $t_2$ ) was used. The source and receiver structures listed in Tables 2 and 3 were used. A water depth of 2 km was considered in the source structure for the offshore earthquake, and the attenuation time constant  $t^*=1$  was used for the P wave.

The source time function and mechanism thus obtained are shown in Figure 3a and 3b. Except for stations CMB, COR, PAB and PAS, the synthetic seismograms determined from this mechanism and source time function can explain the observed waveform very well as shown in Figure 2. Since the stations CMB, COR, PAB and PAS have the epicentral distance of about  $100^\circ$  from the hypocenter (Table 1), the data is less reliable due to the contamination of noise. The mechanism determined from the inversion had plane 1: strike= $135.3^\circ$ , dip= $23.6^\circ$ , rake= $-31.4^\circ$  and plane 2: strike= $254.5^\circ$ , dip= $78^\circ$ , rake= $-250^\circ$ . This mechanism has most of the vertical components of slip with a small amount of strike

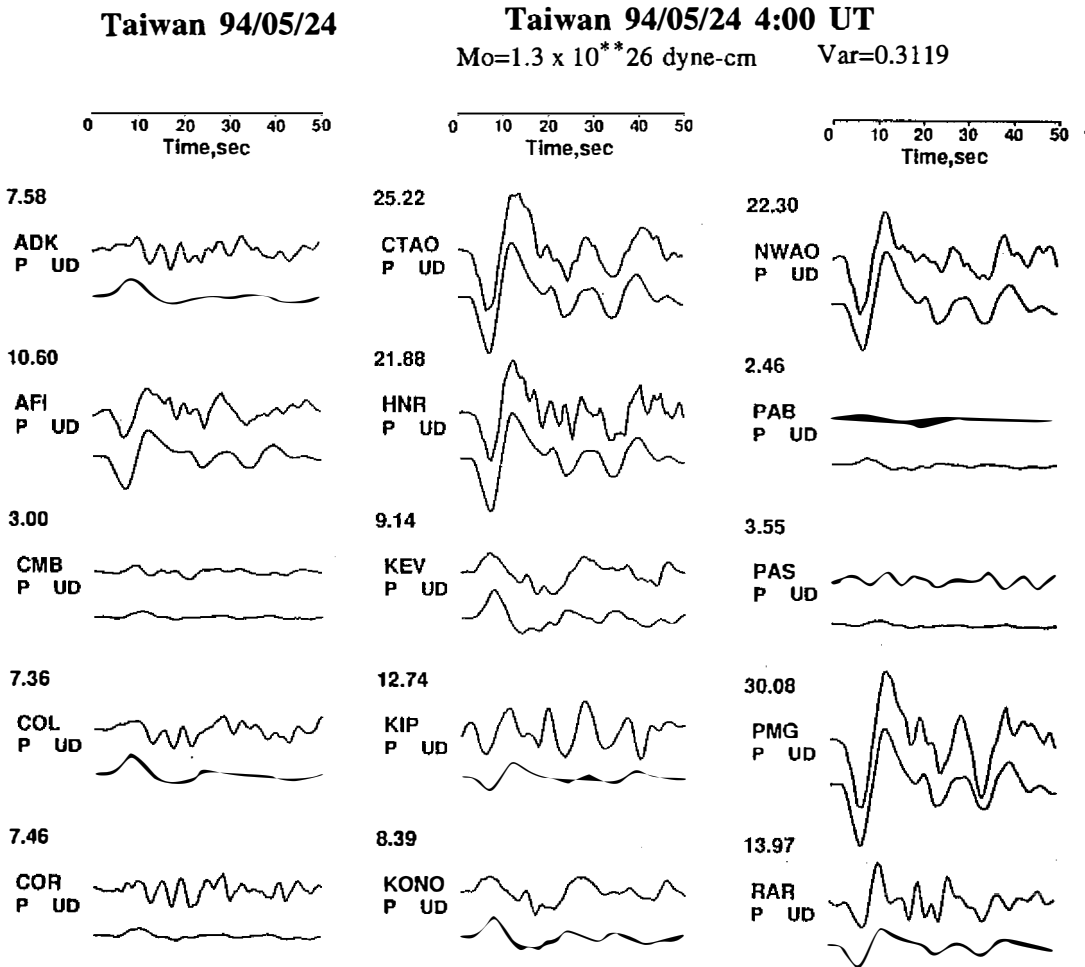


Fig. 2. Observed (top) and synthetic (bottom) seismograms for the 1994 Hualien earthquake. All the records show ground motion displacement. The numbers under the station codes are the absolute displacement amplitudes in  $\mu$ .

slip. The fault plane of the earthquake was difficult to determine. The fault plane with strike of  $135.3^\circ$  and small dipping angle of  $23.6^\circ$  was considered as the fault plane since its strike was more consistent with the strikes of the Ryukyu Trench in the tectonic model as proposed by Bowin *et al.* (1978). The detailed tectonic implications of the earthquake needed to be solved by considering the aftershock data and the mechanisms of the earthquake sequence.

The source time function from the inversion revealed one main event with a source duration of 8.5 sec followed by two small subevent sequences and two distinct subevents. If all the subevents were considered, the total source duration would be 35 sec. The moment for the first main event was  $7.06 \times 10^{25}$  dyne-cm which is similar to the moment of  $6.7 \times 10^{25}$  dyne-cm determined from the Harvard Centroid Moment Tensor (CMT). If all of the later subevents were considered, the total moment of this earthquake would be up to  $1.3 \times 10^{26}$  dyne-cm.

Table 1. 15 stations of the IRIS used in the long-period P-wave inversion for the Hualien earthquake.  $\Delta$ ,  $\phi$ , and  $\phi_B$  denote the hypocentral distance, azimuth and back azimuth, respectively.

Station	$\Delta$ (deg.)	$\phi$ (deg.)	$\phi_B$ (deg.)
ADK	53.6	42.1	-96.9
AFI	74.7	113.2	-59.8
CMB	94.6	44.6	-54.5
COL	68.3	27.2	-79.4
COR	89.0	40.4	-56.3
CTAO	49.9	150.1	-29.0
HNR	49.7	127.8	-47.0
KEV	69.4	-21.6	76.4
KIP	72.5	73.8	-70.5
KONO	80.1	-28.2	58.8
NWAO	57.1	-174.9	5.5
PAB	99.3	-38.8	48.0
PAS	98.3	46.7	-53.5
PMG	41.3	141.1	-35.6
RAR	88.2	114.2	-63.3

Table 2. Source velocity-structure used in the inversion. A two-kilometer depth of water was considered for the offshore events.  $V_p$ ,  $\rho$  and  $H$  denote the P-wave velocity, density and thickness of the layer, respectively.

Source Structure		
$V_p$ (km/sec)	$\rho$ (g/cm <sup>2</sup> )	$H$ (km)
1.50	1.0	2.0
6.50	2.87	20.0
8.10	3.30	---

Table 3. Receiver velocity-structure.  $V_p$ ,  $\rho$  and  $H$  denote the P-wave velocity, density and thickness of the layer, respectively.

Receiver Structure		
$V_p$ (km/sec)	$\rho$ (g/cm <sup>2</sup> )	$H$ (km)
5.57	2.65	15.0
6.50	2.87	18.0
8.10	3.30	---

The fault plane solution shown in Figure 3c was determined by the CMT using 12 IRIS stations. The CMT solution is the Centroid-Moment Tensor (CMT) inversion method developed by Dziewonski *et al.* (1981). An earthquake with a seismic moment larger than  $5 \times 10^{23}$  dyne-cm was routinely determined by the Harvard CMT group. The fault planes of the CMT solution show two similar strikes fault planes but one with a near vertical dipping plane and the other with a small dipping plane toward to the southeast. The difference between

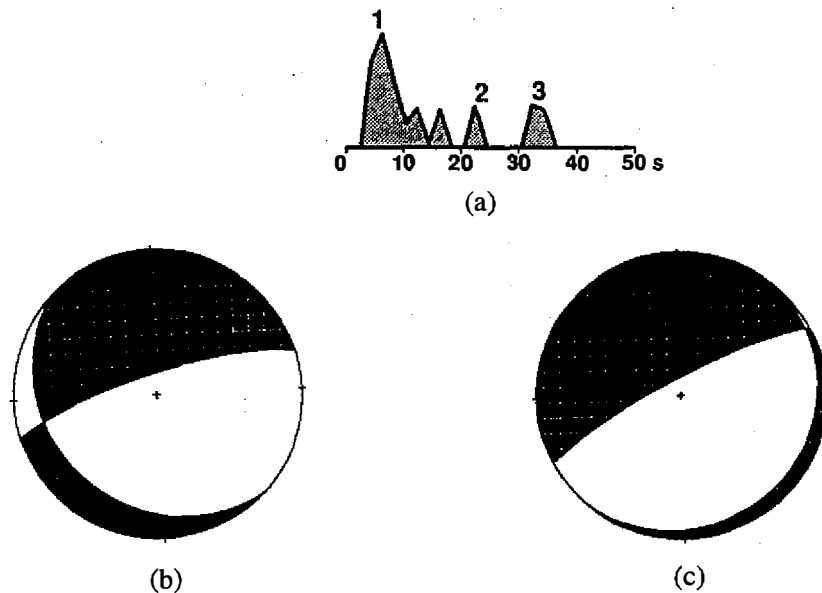


Fig. 3. (a) Resulting source time-function and (b) mechanism determined from long period body wave inversion. (c) Mechanism determined by the Harvard CMT.

the CMT solution and the solution in this study might have resulted from the difference in the period of the wave used which led to a difference in the dip angle.

## 2.2 The 1994 June 5 Nanao Earthquake

The same technique was applied to the 1994, June 5 Nanao earthquake. 7 of IRIS stations were used for this earthquake. The parameters of these 7 stations respect to the epicenter are listed in Table 4. The long period P-wave waveforms of the 7 stations are shown in Figure 4. Except for the WRAB station, for most of the stations with a hypocentral distance less than  $50^\circ$ , the body waveforms show double picks of P-waves. Since these might have been caused by source or structure, we compared the waveforms at stations WRAB, CTAO, HNR and PMG, which have hypocentral distances less than  $50^\circ$  and azimuths of  $125^\circ$  to  $150^\circ$ , for the Hualien and Nanao earthquakes. Because these stations have very similar parameters in terms of hypocentral distance, azimuth and back azimuth with respect to the epicenters of the Hualien and Nanao earthquakes, the ray paths arriving at the stations were considered as have covering almost the same region for both earthquakes. As shown in Figure 2, the P-waves for the Hualien earthquake for those stations do not show the double picks like those for the Nanao earthquake, shown in Figure 4. This discrepancy suggests that the double pick P-waves found in the Nanao earthquake was caused by source but not by the local structure. However, the doublet waveform was not found in the WRAB station for the Nanao earthquake. The reason for this is not clear yet.

We first considered a trapezoidal source time function as shown in Figure 5a to simulate the seismograms. The resulting mechanism is shown in Figure 5b. The synthetic seismograms from the source time function can generally explain the observed waveforms but cannot explain the doublet of the body wave as shown in Figure 4. When a two-triangle source time

Table 4. 7 stations of the IRIS used in the long-period P-wave inversion for the Nanao earthquake.  $\Delta$ ,  $\phi$ , and  $\phi_B$  denote the hypocentral distance, azimuth and back azimuth, respectively.

Station	$\Delta$ (deg.)	$\phi$ (deg.)	$\phi_B$ (deg.)
ARU	55.2	-37.0	97.8
COL	68.1	27.2	-78.8
CTAO	50.5	149.9	-29.1
HNR	50.3	127.8	-46.8
KONO	79.4	-28.4	58.9
PMG	41.9	140.9	-35.5
WRAB	46.1	163.6	-15.8

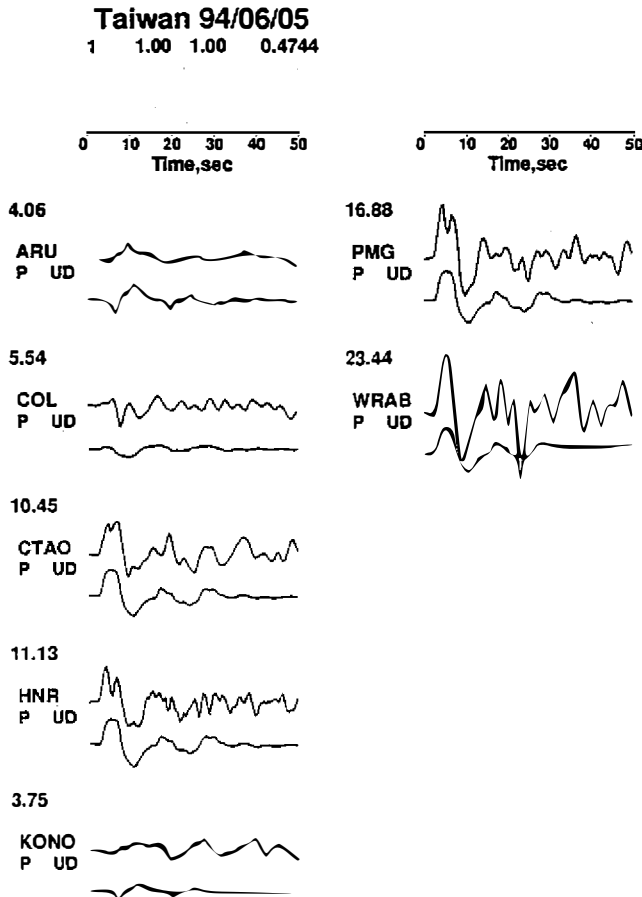


Fig. 4. Observed (top) and synthetic (bottom) seismograms for the 1994 Nanao earthquake. All the records show ground motion displacement. The numbers under the station codes are the absolute displacement amplitudes in  $\mu$ .

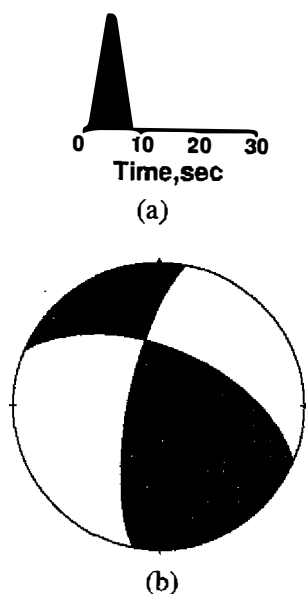


Fig. 5. (a) Trapezoidal source time-function and (b) mechanism determined from long period body wave inversion.

function with a time delay of 2 sec was considered, the doublet body wave could be explained very well. Figures 6a and 6b, in fact, show the source time function and mechanism thus determined. The mechanism shows a strike slip focal mechanism (dip= $62.6^\circ$ , rake= $25.0^\circ$  and strike= $293.2^\circ$ ), which is similar to the Harvard CMT solution (dip= $61^\circ$ , rake= $-3^\circ$  and strike= $271^\circ$ ) shown in Figure 6c. As a means of comparison with the observed seismograms, the synthetic seismograms obtained from this solution are shown in Figure 7.

The source time function of the Nanao earthquake is much simpler than that of the Hualien earthquake although they have similar magnitudes. A doublet source time function can simply explain the observed seismograms well. This doublet source time function has the moment of  $3.73 \times 10^{25}$  dyne-cm which is comparable to that,  $3.9 \times 10^{25}$  dyne-cm, of the CMT solution.

### 3. GEOMETRY OF THE FAULT

The source time function determined from long period P-waves can be interpreted in terms of the slip distribution along the fault. Here, we interpretate it using a modified Haskell (1964) model which had been used to determine the slip distribution of the 1992 Landers, California, earthquake by Kanamori *et al.* (1992). To compute the slip distribution along the fault, the geometry of the fault must be estimated.

#### 3.1 The 1994 May 24, Hualien Earthquake

The depth of the Hualien earthquake as determined by the CWBSN using local seismography network data is 2.9 km, but determined from the long period P-waves is 12 km and 9 km from the CMT. In the present study, the depth of 2.9 km is considered as the upper depth of the fault and 9 km as the centroid depth of the fault. This yields a fault width of 12 km which is consistent with the depth determined from the long period P-waves.

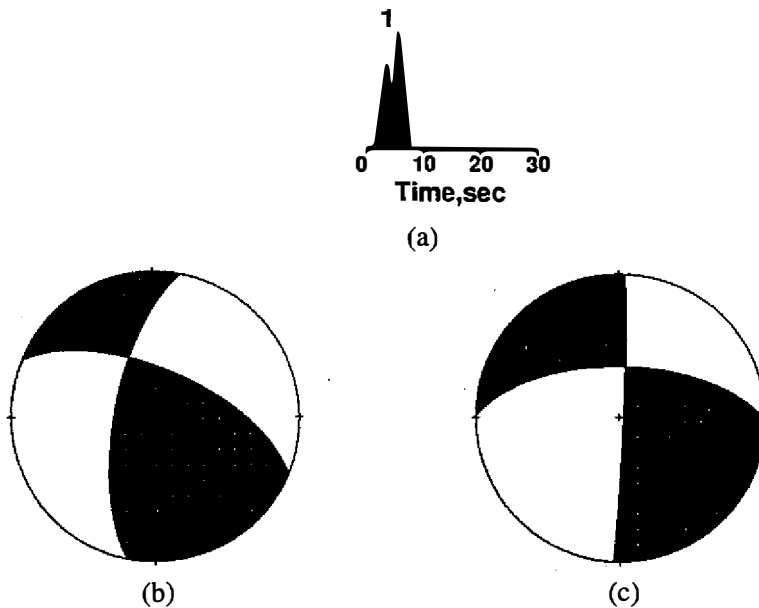


Fig. 6. (a) Two-triangle source time-function and (b) mechanism determined from long period body wave inversion. (c) mechanism determined by the Harvard CMT.

We assumed an unilateral rupture of the fault and the rupture velocity of  $V=2.5$  km/sec. If the effective duration of the source,  $\tau$ , of 8.5 sec was considered (Main event), the rupture length of the fault could be approximated by  $L=V\tau=21.25$  km. If the total source duration of 35 sec was considered, the rupture length of the fault would be up to 87.5 km. If this rupture length was considered, the heterogeneity slip distribution on the fault could be expected from the source time function. The rupture length of 21.25 km can be considered as the largest asperity on the fault plane. The other small subevents are small asperities randomly distributed over the fault plane. If the rigidity of  $\mu=3 \times 10^{11}$  dyne/cm<sup>2</sup> was assumed, an average slip of 92.3 cm would be obtained in this large asperity. This average slip would be reduced if larger asperity were considered. The average slip of 91.5 cm and 40 cm on the fault would be obtained, respectively, if the sequential events and the two later distinct subevents followed by the main event were considered.

### 3.2 The 1994 June 5 Nanao Earthquake

The depth of the Nanao earthquake determined from the CWBSN using local seismography network data is 5.3 km, but if it was determined from this long period P-wave, it would be 12 km and 15.9 km from the CMT. Using a similar estimation to the one made in the previous section, the fault width was approximated to be about 16 km.

We also assumed an unilateral rupture of the fault with a rupture velocity of  $V=2.5$  km/sec. If the effective duration of the source,  $\tau$ , was 6 sec, the rupture length of the fault would be  $L=V\tau=15$  km which would yield an average slip of 51.8 cm on the fault if the rigidity of  $\mu=3 \times 10^{11}$  dyne/cm<sup>2</sup> was considered. However, the similarity of fault length and width suggests the Nanao earthquake might have resulted from a circular fault. If a circular fault model was considered, the slip amount on the fault would change accordingly.

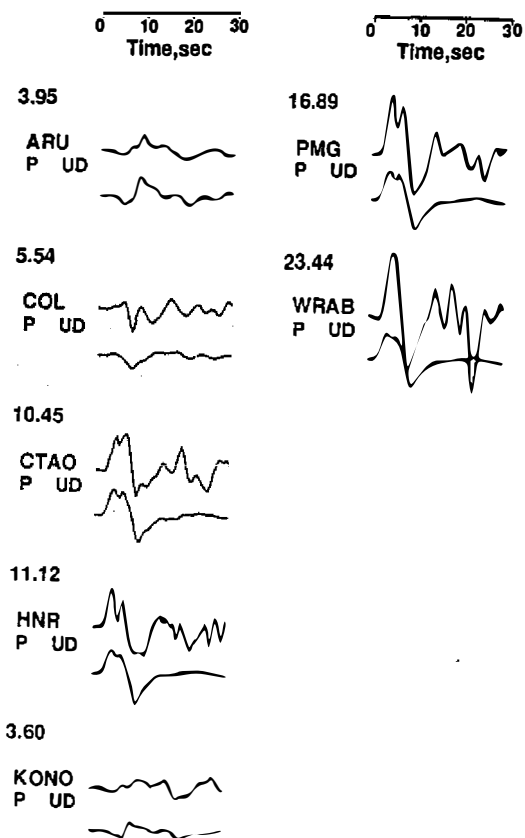


Fig. 7. Comparison of the synthetic seismograms (bottom) from a two-triangle source time-function (Figure 6) and observed seismograms (top).

#### 4. MAGNITUDE, TSUNAMI AND STRESS DROP

The 1994 May 24 Hualien earthquake has many different magnitude scales. The local magnitude of the earthquake determined from the CWBSN is 6.2. The body wave and surface wave magnitude determined by the Harvard CMT solution is  $m_b=5.9$  and  $M_s=6.6$ . The moment magnitude using  $M_w=(\log M_0/1.5)-10.7$  (Kanamori, 1978) is 6.5 from the CMT and  $M_w=6.6$  for the long period P-wave. Essentially, this earthquake contained most of the long period energy which can even be understood from personal experience during the earthquake. The difference between the  $m_b$  and  $M_s$  from the Harvard CMT implies this earthquake generated a larger amount of surface waves than body waves.

Kanamori and Anderson (1975) considered an earthquake a slow earthquake if its  $L/V_r$  is greater than  $T_0/\pi$ , where  $L/V_r$  is the rupture time and  $T_0=20$  sec which is the typical period used for determining the surface wave magnitude. The Hualien earthquake's rupture time is 8.5~35 sec which is much larger than  $T_0/\pi=6.37$  suggests that this earthquake is a slow earthquake.

An offshore slow earthquake is usually a tsunami-generating earthquake (Kanamori and Kikuchi, 1993). The 1994 Hualien earthquake occurred near the location (122.6°E, 24.1°N)

of the 1966 Hualien earthquake ( $M=7.5$ ) which generated large tsunami and killed 7 people (Ye, 1993). The slow earthquake of the Hualien earthquake increases the possibility of its generating of tsunami.

Kanamori and Kikuchi (1993) suggest the diagnostic feature for a tsunami earthquake from the difference between the  $M_s$  and  $M_w$ , since the  $M_w$  is usually much larger than the  $M_s$  for a tsunami earthquake, e.g. the 1992 Nicaragua earthquake had  $M_w=7.6$  but  $M_s=7.0$ . The similarity between the  $M_w$  and  $M_s$  for the Hualien earthquake implies this earthquake was not a tsunami earthquake although some minor tsunamis were found in some locations. The Japanese Meteorological Agency (JMA) made a tsunami warning along the southwestern coast of Japan during the Hualien earthquake, but no tsunami hazards were reported. The mechanism of the 1994 Hualien earthquake was very similar to that of the 1992 Nicaragua earthquake (Kanamori and Kikuchi, 1993). However, the 1992 Nicaragua earthquake generated abnormal tsunamis which were not found in the 1994 Hualien earthquake. This difference might have been due to the almost an order difference in  $M_w$  and the difference in the subducting environments of these two earthquakes. This discussion increases the awareness of the possibility of a tsunami hazard in Hualien City if an earthquake in a similar location but with a larger magnitude than the 1994 Hualien event occurred.

Although the June 5 Nanao earthquake was also an offshore earthquake, the strike slip focal mechanism reduced the possibility of tsunami generation (Ma, 1993). The similar magnitude scales of  $M_s$  (6.2),  $M_w$  (6.4) and  $M_L$  (6.2) suggest the Nanao earthquake was just a typical earthquake.

Since the 1994 Hualien and Nanao earthquakes can be considered plate margin earthquakes, they were compared with 41 other large earthquakes in the world which were used by Kanamori and Anderson (1975) for stress drop estimation. Based on the seismic moment and the geometry of the fault estimated from the previous sections, for the Hualien earthquake, there was a stress drop of about 50 bars for  $M_0=7.06 \times 10^{25}$  dyne-cm and  $S=L \times W=21.25 \times 12 \text{ km}^2=225 \text{ km}^2$  and, for the Nanao earthquake, a stress drop of about 30 bars for  $M_0=3.73 \times 10^{25}$  dyne-cm and  $S=L \times W=15 \times 16 \text{ km}^2=240 \text{ km}^2$  (Figure 8). The stress drops of the earthquakes are consistent with the observation of other large inter-plate earthquakes. If the moment of  $1.3 \times 10^{26}$  dyne-cm and  $S=L \times W=87.5 \times 12 \text{ km}^2=1050 \text{ km}^2$  are considered for the Hualien earthquake, the stress drop of 10 bar would be obtained. This stress drop is smaller than the average stress drop of most inter-plate events (30 bars), but within the range of 10 bars and 100 bars for shallow earthquakes observed by Chinnery (1964) and Aki (1972).

## 5. CONCLUSIONS

The solution based on teleseismic body waves gives a mechanism with  $\text{dip}=23.6^\circ$ ,  $\text{rake}=-31.4^\circ$  and  $\text{strike}=135.3^\circ$ , and a seismic moment of  $9.0 \times 10^{25} \sim 1.3 \times 10^{26}$  dyne-cm ( $M_w=6.6 \sim 6.7$ ) for the Hualien earthquake; and with  $\text{dip}=62.6^\circ$ ,  $\text{rake}=25.0^\circ$  and  $\text{strike}=293.2^\circ$ , and a seismic moment of  $3.73 \times 10^{25}$  dyne-cm ( $M_w=6.4$ ) for the Nanao earthquake. The source time function of the May 24, 1994 Hualien earthquake consists of a main event with a time duration of 8 sec followed by two small subevents which extend the total duration of the source time function to 35 sec. This long duration of source time function and the difference between  $M_s$  and  $m_b$  suggest this earthquake is a slow earthquake. The source time function of the June 5, 1994 Nanao earthquake has a time duration of 6 sec and is rather simple to

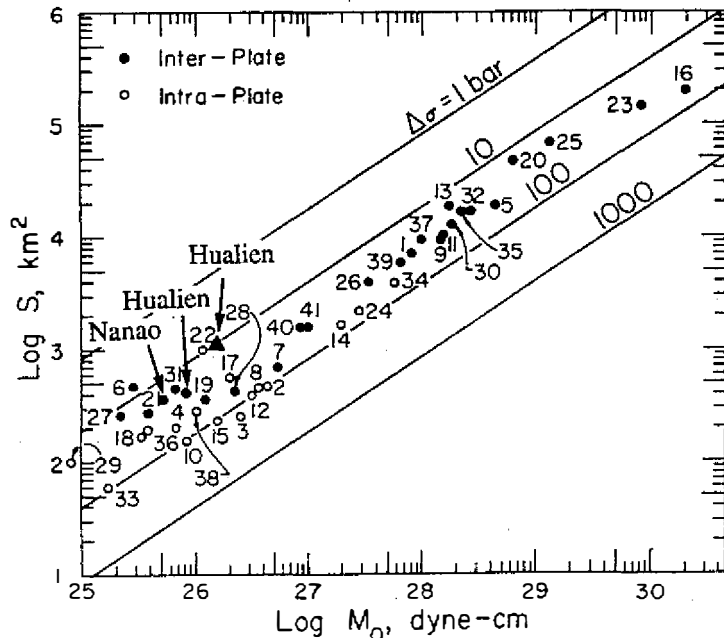


Fig. 8. Relation of  $S$  (fault surface area) and  $M_0$  (seismic moment) for the 1994 Hualien and Nanao earthquakes and 41 other large events taken from Kanamori and Anderson (1975). The triangle symbol denotes the Hualien event for the fault model with a long source duration time of 35 sec. The straight lines give the relations for circular cracks with a constant  $\Delta\theta$  (stress drop).

compare with that of the Hualien earthquake. The average slips on the fault for the Hualien and Nanao earthquakes are 40~92.3 cm and 51.8 cm, respectively. The stress drops of the two intra-plate events are comparable to most of the observations for other large earthquakes world-wide.

**Acknowledgments** The authors wish to thank the IRIS Data Management Center for providing open access to regional distance waveforms for this type of rapid analysis. The discussions held with Dr. H. Kanamori and J. H. Wang were very much appreciated.

## REFERENCES

- Aki, K., 1972: Scaling law of earthquake source time-function. *J. Geophys.*, **31**, 3-25.  
 Bowin, C, R. S. Lu, C. S. Lee, and H. Schouten, 1978: Plate convergence and accretion in Taiwan-Luzon region. *Bull. Am. Assoc. Petrol. Geol.*, **62**, 1645-1672.  
 Chinnery, M. A., 1964: The strength of the earth's crust under horizontal shear stress. *J. Geophys. Res.*, **69**, 2085-2089.

- Dziewonski, A. M., T. A. Chou, and J. H. Woodhouse, 1981: Determination of earthquake source parameters from waveform data for studies of global and regional seismicity. *J. Geophys. Res.*, **86**, 2825-2852.
- Haskell, N., 1964: Total energy and energy spectral density of elastic wave radiation from propagating faults, 2. *Bull. Seism. Soc. Am.*, **56**, 1811-1842.
- Kanamori, H., and D. L. Anderson, 1975: Theoretical basis of some empirical relations in seismology. *Bull. Seism. Soc. Am.*, **65**, 1073-1095.
- Kikuchi M., and H. Kanamori, 1982: Inversion of complex body waves. *Bull. Seism. Soc. Am.*, **72**, 491-506.
- Kikuchi M., and H. Kanamori, 1986: Inversion of complex body waves-II. *Phys. Earth Planet. Inter.*, **43**, 205-222.
- Kikuchi M., and H. Kanamori, 1991: Inversion of complex body waves-III. *Bull. Seism. Soc. Am.*, **81**, 2335-2350.
- Kikuchi M., and H. Kanamori, 1993: The 1992 Nicaragua earthquake: a slow tsunami earthquake associated with subducted sediments. *Nature*, **361**, 714-716.
- Kanamori, H., H.-K. Thio, D. Dreger, and E. Hauksson, 1992: Initial investigation of the Landers, California, earthquake of 28 June 1992 using TERRAScope. *Geophys. Res. Lett.*, **19**, 2267-2270.
- Ma, K.-F., 1993: Part I: The origin of Tsunamis excited by local earthquakes. California Institute of Technology, Ph. D. Thesis, 219pp.
- Wu, Francis T., 1970: Focal mechanisms and tectonics in the vicinity of Taiwan. *Bull. Seism. Soc. Am.*, **60**, 2045-2356.
- Wu, Francis T., 1978: Recent tectonic of Taiwan. *J. Phys. Earth*, **26**, Suppl. S265-S299.
- Ye, L., X. Wang, and C. Bao, 1993: Tsunami in the China Sea and its warning service. *Proc. Tsunami Sym.*, 771-778.